



# Computational study of the CO adsorption and diffusion in zeolites: validating the Reed–Ehrlich model

Vladimir Berezovsky<sup>1</sup> · Sven Öberg<sup>2</sup>

Received: 9 November 2017 / Revised: 22 March 2018 / Accepted: 3 April 2018 / Published online: 28 April 2018  
© The Author(s) 2018

## Abstract

Molecular simulations have been employed to explore at the microscopic scale the adsorption of CO in zeolites (MFI, CHA and DDR). On the basis of classical force fields, grand canonical Monte Carlo simulations are performed to predict the adsorption properties (isotherms) of these types of zeolites up to high pressure. Subsequent careful analysis yields details the microscopic mechanism in play, along the whole adsorption process, together with a considering of the arrangements of CO in MFI at high pressure. This work also summarizes an approach which uses single component diffusion data in prediction of multicomponent diffusion.

**Keywords** Adsorption · Diffusion · Zeolite · Carbon monoxide · Grand canonical Monte Carlo · Molecular dynamics

## 1 Introduction

Synthetic gas, or syngas, is used for the production of fuel such as methanol and dimethyl ether (Gądek et al. 2013; Azizi et al. 2014). Syngas can be made from various raw materials (Richardson et al. 2015) such as, for example, black liquor. Black liquor is a by-product of wood-pulp production that contains the process chemicals and biomass in the form of wood residues. Methanol is generated from carbon monoxide, carbon dioxide, and hydrogen contained in syngas using a catalyst based on oxides of copper and zinc (Marschner and Moeller 1983). Syngas also contains other components, including various by-products, in addition to these three gases. To prevent deactivation of the sensitive catalyst, the process gas must be purified before entering

the reactor for methanol production (Knoef 2005). Carbon monoxide has strong reducing properties, and is particularly useful for industrial applications, such as production of methane, alcohols, organic acids and esters. In contrast to these uses, its well known toxicity for hemoglobin animals, makes it an undesirable atmospheric pollutant, particularly in industrialized areas. Oxides of carbon are involved in many chemical and industrial processes, and their removal to prevent them from harming the environment thus is, naturally, a matter of concern. Selective adsorption of the carbon oxides for purifying hydrogen produced from syngas, also has economic benefits (Liu et al. 2010).

Carbon monoxide is the product of incomplete combustion of a carbonaceous fuel, and as such is inevitably found at varying concentrations in all exhaust streams. At present, there are two methods available by which CO may be separated from a mixture of exhaust gases for subsequent use it as a chemical reagent: chemical reactions and liquefaction (Eller and Frederick 1949).

Liquefaction is applicable only in the case where a gas mixture containing CO has a relatively low concentration of nitrogen, due to the complexity of separating CO from a large amount of nitrogen by liquefaction. Such gas mixtures should also be substantially free of water vapour and carbon dioxide, because these compounds form solid phases at the temperatures involved in the liquefaction process, which may cause obstructions in the plant [Liquefaction of Gases, The

**Electronic supplementary material** The online version of this article (<https://doi.org/10.1007/s10450-018-9948-z>) contains supplementary material, which is available to authorized users.

✉ Vladimir Berezovsky  
v.berezovsky@narfu.ru

<sup>1</sup> Department of Applied Mathematics and High-performance Computing, M.V.Lomonosov Northern (Arctic) Federal University, Severnaya Dvina Emb. 17, Arkhangelsk, Russia 163002

<sup>2</sup> Division of Materials Sciences, Department of Engineering Sciences and Mathematics, Luleå University of Technology, Luleå, Sweden

Great Soviet Encyclopedia, 3rd edn, The Gale Group, Inc., Farmington Hills (1970–1979)].

Various purification techniques to remove unwanted compounds may be used prior to the manufacture of methanol or dimethyl ether (Dragomirova et al. 2015; Feng et al. 2015). One of the most promising technologies employs inorganic membranes based on functional coatings to create a chemical environment in the form of a microporous zeolite coating (Dragomirova et al. 2015; Feng et al. 2015; Ackley et al. 2003). Zeolites generally stand out as the most advantageous and competitive porous solids used for industrial applications based on physisorption for the selective capture of selected gases. It shows high permeability and selectivity, with sufficient thermal and chemical stability, which allows the integration of membrane processes for the cost-effective production renewable fuels and chemicals (Ackley et al. 2003).

Recently, several developments relating in general to methods for recovery of CO from gas mixtures, and in particular to a process of selectively adsorbing CO from gas mixtures using a zeolite sieve effect (Sethia et al. 2013). Accurate description of the properties of adsorption and diffusion of molecules in zeolite membranes for gas mixtures plays an important role in the engineering of processes for separating mixtures. Optimization of the operating conditions for zeolitic membranes is aided by developing a detailed understanding of the adsorption and diffusion processes that are involved. It has been found that the mass transfer of CO<sub>2</sub> and H<sub>2</sub> in an MFI zeolite can be described by a Maxwell–Stefan (MS) model (Taylor and Krishna 1993; Krishna and Broeke 1995). By applying this model data of single-component adsorption and diffusion can be used to predict the gas mixture separation with a high degree of confidence (Dubbeldam and Snurr 2007).

MS approach for modeling the performance of zeolite membranes in separations has proven to be useful. It allows to predict the mixture permeances based on single component adsorption and diffusion data as an input to the model. Recently, a model of the transport through the composite membrane structure was described (Grahn and Hedlund 2014), where transport through the zeolite layer assumed to occur both via zeolite pores and via flow-through defects. Maxwell–Stefan formalism (Taylor and Krishna 1993; Krishna 2014) in combination (Kapteijn et al. 2000) with the ideal adsorbed solution theory (IAST) was implemented to describe transport through the zeolite pores.

Zeolite membranes are an attractive instrument for gas separation due to the high flux capability and its chemical, mechanical and thermal stability. Having well-defined pore structure these membranes can facilitate high selectivity. Despite it has been found more than 200 different zeolite structures, just few of them can be prepared as a membranes, in particular MFI (Guo et al. 2006; Sandström et al. 2011;

Bernal et al. 2004), CHA (Hong et al. 2008; Li et al. 2006), DDR (Himeno et al. 2007; Tomita et al. 2004), LTA (Sato et al. 2008a, b), FAU (Caro and Noack 2008; Kusakabe et al. 1999) and SOD (Julbe et al. 2003; Khajavi et al. 2009). Worse yet, most of them have a low permeability by the reason of the high film thickness and moderate selectivity by the reason of defects.

MFI membranes possess efficient separation of small gas molecules utilizing adsorption selectivity inspite the molecular sieving (Kosinov et al. 2016) due to the average pore size of MFI zeolite (5.5 Å) is larger than kinetic diameter of those molecules. On the contrary DDR membranes with window size by 3.6 × 4.4 Å can separate small gas molecules based on molecular sieving, for example selectivity for CO<sub>2</sub>/CH<sub>4</sub> is 100–3000 (Bergh et al. 2008). Similar high selectivity can be achieved utilizing CHA (3.8 Å) membranes (Li et al. 2006). However, small pore membranes such as DDR and CHA, have the low membrane permeance by present manufacture methods.

Owing to the flammability and high toxicity of carbon monoxide making it a difficult material to study in experiments, there is relatively little information on its adsorption and diffusion in zeolites. Indeed, the high toxicity of carbon monoxide creates considerable problems for making gravimetric, manometric, and microcalorimetric measurements, emphasising the need to involve computational methods to predict thermodynamic properties of such systems. In the present work, molecular simulations are used to predict the adsorption properties of CO in the MFI, CHA, and DDR types of zeolites, and its diffusion behaviour in MFI. We also examine the applicability of the Reed–Ehrlich model for calculating diffusivities in zeolites (Reed and Ehrlich 1981).

In general, where the transport diffusivity no longer takes the form of Henry's law, it increases strongly with the loading due, mainly to the dominant effect of thermodynamic correction factor, which for a suitable adsorption isotherm increases strongly after saturation (Kärger et al. 2012). Of particular interest are corrected diffusion coefficients computed from the transport diffusion coefficients. According to the Reed–Ehrlich model, the dependence of corrected diffusivity on loading is much weaker than the same dependence for the Fickian diffusivity for a wide variety of different systems, and corrected diffusivity, as found experimentally, is approximately independent from the loading, except in the saturation region (Kärger et al. 2012) [see detailed discussion also at Dubbeldam and Snurr (2007)].

However, the definition of the thermodynamic factor requires very accurate equilibrium isotherms, especially at high adsorption value where it is exposed to significant volatility. Corrected diffusivity is dependent on the loading, and thus can experimentally be observed only when the variation is relatively large. Since the Reed–Ehrlich model is based on a lattice model, it implies that with saturation the corrected

diffusivity must decay to zero. However, as the thermodynamic factor tends to infinity, the Fickian diffusivity corresponding to the product of the mobility (jump rate) and thermodynamic factor, tends to a finite limit. When there is no interaction, then Fickian diffusivity is independent of the loading. Although the experimental data at high loading are limited, the sharp decline in diffusivity is widespread, especially for systems with open pores, but the observed decline is usually not as sharp as the model predicts. In fact, one can expect that for saturated diffusion in systems with open pores will drop to a certain part of the liquid phase diffusion under similar conditions other than zero (Kärger et al. 2012).

## 2 Methodology

Most of the published molecular simulation studying in zeolites at this time have used Kiselev's model (1978). In this model zeolite atoms are fixed, and interactions of guest atoms with silicon atoms is accounted for by an effective interaction only with the surrounding oxygen atoms. This model has shown a significant success, both in using the molecular dynamics method to compute the diffusivities via the Einstein relation (Dubbeldam and Snurr 2007), and using the Monte Carlo method to calculate the sorption of hydrocarbons (Xu et al. 2007).

Adsorption of carbon monoxide was investigated by a Monte Carlo method for a grand canonical ( $\mu$ VT) ensemble using the MCCCSTowhee (Martin 2013) program for rigid framework models of MFI. This Monte Carlo molecular simulation tool includes the configurational-bias Monte-Carlo (CBMC) algorithm. Two model systems are used in the present work: adsorbent and adsorptive reservoir. In these, the probabilities for GCMC moves involving CO particles are as follows: insertion/deletion 50%; translation 25%; intrabox reinsertion 25%. For each chemical potential,  $10^7$  steps are used to equilibrate the system, and a further  $10^7$  are used for data collection. The Towhee code requires analytical values for chemical potentials rather than pressures as input. In this work, we use GCMC simulations (one simulation box only) in the isobaric-isothermal (NpT) ensemble to determine the pressure of CO at a given chemical potential.

The orthorhombic phase ( $Pnma$  space group) of MFI zeolite is used as the basis for the simulations of this material. Its crystallographic parameters are  $a = 20.0511 \text{ \AA}$ ,  $b = 19.8757 \text{ \AA}$ ,  $c = 13.3682 \text{ \AA}$ , where  $a$  is main direction of zigzag, and  $b$  is direction of the straight channels. The simulation cell comprises  $2 \times 2 \times 3$  unit cells. For pure silica chabazite (CHA) the model crystal is rhombohedral ( $R3m$ ) with  $a = 13.675 \text{ \AA}$ ,  $b = 13.675 \text{ \AA}$ ,  $c = 14.767 \text{ \AA}$ , and the simulation cell comprises  $3 \times 3 \times 2$  unit cells. The all-silica DDR zeolite is also rhombohedral  $R3m$ , and its lattice parameters are  $a = 13.795 \text{ \AA}$ ,  $b = 13.795 \text{ \AA}$ ,  $c = 40.750 \text{ \AA}$ . In this instance,

the simulation cell comprises  $3 \times 3 \times 1$  unit cells. The initial atomic positions are provided by Baerlocher and McCusker (2000). The charge assignments for the atoms in the zeolite framework taken from Dubbeldam et al. (2004); García-Pérez et al. (2007) are  $2.05e$  and  $-1.025e$  for Si and O atoms, respectively. The 'bond increment' (Maple et al. 1994) method of charge assignment is used for the framework. The polar model of carbon monoxide (Pałucha et al. 2004) uses two different Lennard-Jones centres, and two partial charges, each with a magnitude of  $0.0223e$ , and separated by the experimentally determined bond length of  $1.128 \text{ \AA}$  (Gilliam et al. 1950). The sign of the charges is negative on the oxygen atom and positive on the carbon atom; thus, the molecule possesses a dipole of  $0.12 \text{ D}$ , which is very close to the experimental value. The Lennard-Jones parameters are  $\sigma = 3.55 \text{ \AA}$  and  $\epsilon/k_B = 37.15 \text{ K}$  for carbon atoms, and  $\sigma = 2.95 \text{ \AA}$  and  $\epsilon/k_B = 61.57 \text{ K}$  for oxygen atoms. The Lorentz-Berthelot rules (Allen and Tildesley 1989) for the mixing interaction then yield  $\sigma = 3.25 \text{ \AA}$  and  $\epsilon/k_B = 47.87 \text{ K}$  for C–O.

An earlier study (García-Pérez et al. 2007), which used a direct Gibbs-ensemble Monte Carlo simulation to calculate the distribution of CO molecules in sI clathrate, similarly employed Lennard-Jones potentials. In this instance, the parameters describing the interactions between carbon atoms and oxygen atoms in the molecules, with the oxygen atoms in the framework, were  $\sigma = 2.7815 \text{ \AA}$ ,  $\epsilon/k_B = 50.2 \text{ K}$ , and  $\sigma = 2.9195 \text{ \AA}$ ,  $\epsilon/k_B = 84.93 \text{ K}$ , respectively. The range of Coulomb and van der Waals interactions are confined to a distance  $r_{cut} = 12 \text{ \AA}$ , beyond which analytical tail corrections are applied. The Ewald summation method is used to calculate the electrostatic interactions (Allen and Tildesley 1989).

For the pressures in the range  $10^2$ – $10^7 \text{ Pa}$ , when mostly one category of the sorption sites are occupied, the simulations are fitted to the ordinary Langmuir–Freundlich (1) and Toth (2) models:

$$N = N_m \frac{bP^\gamma}{(1 + bP^\gamma)}, \quad (1)$$

and

$$N = N_m \frac{bP}{[1 + (bP)^t]^{\frac{1}{t}}}. \quad (2)$$

Also adsorption isotherm obtained by CBMC is fitted to dual-site Langmuir–Freundlich model (Ruthven 1984):

$$N = N_{m_1} \frac{b_1 P^{\gamma_1}}{(1 + b_1 P^{\gamma_1})} + N_{m_2} \frac{b_2 P^{\gamma_2}}{(1 + b_2 P^{\gamma_2})}. \quad (3)$$

The dual-site Langmuir–Freundlich model distinguishing two categories of different active sorption sites in the adsorbent.

The molecular dynamics (MD) simulations for reproducing of diffusion of carbon monoxide molecules in differently loaded zeolite framework are performed using the DL\_POLY program package (Todorov and Smith 2011). The MD simulations begin from equilibrium configurations, which are derived from Monte Carlo simulations. These are subsequently equilibrated for 100 ps, before commencing a 2-ns simulation run. The velocity Verlet algorithm is used for integrating the equations of motion in which a time step of 1 fs is used, in conjunction with a NVT Nose-Hoover thermostat for controlling the temperature, with  $\tau_t = 1$  ps.

The diffusivity for any given conditions can be calculated from the mean-square displacement (MSD) or the velocity auto-correlation function, using the Einstein relation (1905),

$$D_{self} = \frac{1}{6} \lim_{\Delta t \rightarrow \infty} \frac{1}{\Delta t} \frac{1}{n} \sum_{i=1}^n \left\langle (\mathbf{r}_i(t + \Delta t) - \mathbf{r}_i(t))^2 \right\rangle. \quad (4)$$

The term between angled brackets is the ensemble average, where  $\mathbf{r}(t)$  is an initial location of an individual molecule, and  $\mathbf{r}(t + \Delta t)$  is its position after an interval  $\Delta t$ . Thus, the formula represents the kinetic behaviour of each molecule among all the others.

The streaming properties, meaning the collective behaviour of the system, is calculated using the mean square displacement of the centre of mass of the swarm of  $N$  molecules. This corresponds to the corrected diffusivity (Papadopoulos et al. 2004) or Maxwell–Stefan diffusivity using (Krishna Skoulidas et al. 2003; Krishna 2009) definition:

$$D_0 = \frac{1}{6} \lim_{\Delta t \rightarrow \infty} \frac{1}{\Delta t} \left\langle \left( \frac{1}{n} \sum_{i=1}^n (\mathbf{r}_i(t + \Delta t) - \mathbf{r}_i(t)) \right)^2 \right\rangle. \quad (5)$$

$D_0$  is a collective property, and has much poorer statistics than  $D_{self}$ .

### 3 Results and discussion

Our Monte Carlo simulations yield adsorption isotherms for CO at 278, 298, and 318 K. The results are shown in Fig. 1

Adsorption isotherms obtained by the Configuration-bias Monte-Carlo method in a Grand canonical ensemble can be compared by fitting them to empirical adsorption models. In some zeolite structures, such as MFI, straight channels are connected via zig-zag channels, forming a network where different adsorption locations can be distinguished between those that lie within the channel interior, and ones at the intersections joining the straight and zig-zag channels. These isotherms generally give rise to an inflection corresponding to the saturation

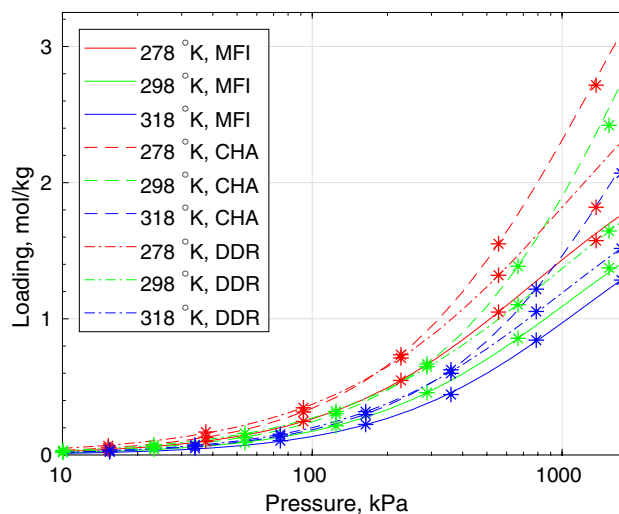


**Fig. 1** Computed adsorption isotherms of CO in MFI (solid line), CHA (dash-dotted line) and DDR (dashed line) at 278 K (red), 298 K (green) and 318 K (blue), fitted using the Langmuir–Freundlich model (1). (Color figure online)

of the first type of adsorption sites. Langmuir–Freundlich isotherms are represented by Eq. (1).

The pressure range  $10^2$ – $10^6$  Pa is of greatest interest in terms of practical use, see Grande (2012) and references therein. Fitting the adsorption isotherms in the regime where Henry’s law applies gives the parameters for the Langmuir–Freundlich (1) and Toth (2) models shown in Table 1. Despite combining features of both Langmuir and Freundlich models, the Langmuir–Freundlich isotherm still does not follow the expected linear behaviour at low pressures. The Toth isotherm, in contrast, does satisfy both the low and high pressure limits. In this work adsorption isotherm has also been fitted for dual-site Langmuir–Freundlich model (Ruthven 1984) over the pressure range  $10^2$ – $10^{12}$  Pa, which yields the parameters presented in Supplementary Table S3. From the adsorption isotherm graphs one can see that considered zeolites shows uptake rate in correspondence with their total pore volumes 0.242, 0.321 and  $0.434 \text{ cm}^3 \text{ g}^{-1}$  for MFI, DDR and CHA, respectively (First et al. 2011). Figure 2 compares the simulated isotherms for CO in MFI with the experimental isotherms of Calero and coworkers (2014) and Golden and Sircar (1994). It shows good agreement with experiment in all range of pressures especially for Calero’s simulations (Matito-Martos et al. 2014) at 298 K.

The Clausius–Clapeyron Eq. (6) yields values for the isosteric enthalpy of adsorption.

$$Q_{st} = -R \left( \frac{\partial \ln (P/P_0)}{\partial T^{-1}} \right)_{c=const}, \quad (6)$$

where  $P$  is the pressure,  $P_0$  is an arbitrary reference pressure,  $T$  is the absolute temperature,  $c$  is the loading, and  $R$

**Table 1** Langmuir–Freundlich and Toth model constants of carbon monoxide adsorption in DDR, CHA and MFI zeolites

	Langmuir–Freundlich constants				Toth constants			
	$N_m$ (mol kg <sup>-1</sup> )	$b$	$\gamma$	Residual	$N_m$ (mol kg <sup>-1</sup> )	$b$ (10 <sup>-6</sup> Pa <sup>-1</sup> )	$t$	Residual
<b>MFI (K)</b>								
278	2.5068	0.6505 × 10 <sup>-6</sup>	1.0520	10.57 × 10 <sup>-6</sup>	1.9794	1.3926	1.3976	16.05 × 10 <sup>-6</sup>
298	2.2344	0.4555 × 10 <sup>-6</sup>	1.0535	23.69 × 10 <sup>-6</sup>	1.5870	1.1097	1.5466	14.34 × 10 <sup>-6</sup>
318	2.1535	0.2497 × 10 <sup>-6</sup>	1.0860	335.4 × 10 <sup>-6</sup>	1.7855	0.7685	1.5209	123.6 × 10 <sup>-6</sup>
<b>DDR (K)</b>								
278	3.8558	2.6150 × 10 <sup>-6</sup>	0.9222	164.2 × 10 <sup>-6</sup>	6.7981	0.7577	0.6016	124.6 × 10 <sup>-6</sup>
298	2.6820	1.6676 × 10 <sup>-6</sup>	0.9660	172.8 × 10 <sup>-6</sup>	2.8279	1.1212	0.8855	159.3 × 10 <sup>-6</sup>
318	2.3818	0.6064 × 10 <sup>-6</sup>	1.0361	333.9 × 10 <sup>-6</sup>	2.2057	0.9479	1.1845	218.3 × 10 <sup>-6</sup>
<b>CHA (K)</b>								
278	5.6670	0.4577 × 10 <sup>-6</sup>	1.0296	0.861 × 10 <sup>-6</sup>	3.9435	0.8863	1.3968	1.774 × 10 <sup>-6</sup>
298	6.7254	0.2998 × 10 <sup>-6</sup>	1.0195	8.672 × 10 <sup>-6</sup>	4.8028	0.5151	1.2906	12.37 × 10 <sup>-6</sup>
318	5.3868	0.2850 × 10 <sup>-6</sup>	1.0194	9.896 × 10 <sup>-6</sup>	3.6106	0.5185	1.3558	4.878 × 10 <sup>-6</sup>

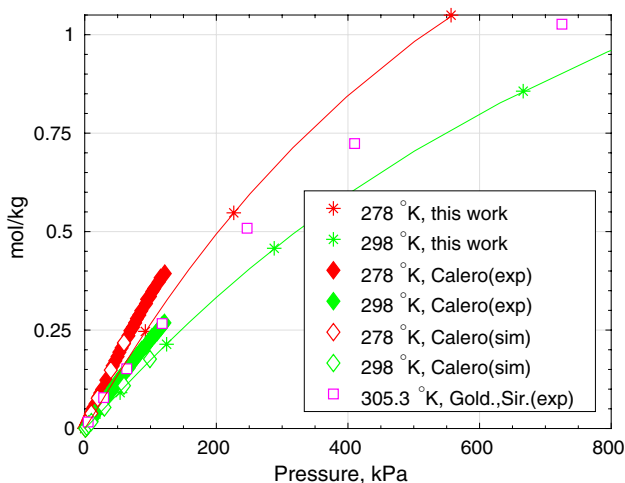


**Fig. 2** Computed adsorption isotherms of CO in MFI-type zeolite (solid line) at 278 K (red), 298 K (green) and 318 K (blue) fitted using the Langmuir–Freundlich (1) model. Experimental (Calero and coworkers 2014; Golden and Sircar 1994) and simulation (Calero and coworkers 2014) data are included for comparison. (Color figure online)

is the gas constant. At low pressures, when for Langmuir–Freundlich parameters  $bP^\gamma \ll 1$  satisfy  $N \approx N_m b P^\gamma$  and from (6) it can be deduced that (7)

$$\begin{aligned}
 Q_{st} &= -R \left( \frac{\partial \ln(P/P_0)}{\partial T^{-1}} \right)_{c=const} \\
 &\approx -R \left( \frac{\partial \ln \left( \left( \frac{N}{N_m b} \right)^{1/\gamma} / P_0 \right)}{\partial T^{-1}} \right)_{N=const} \\
 &\approx R \frac{\Delta \left( \frac{1}{\gamma} \ln N_m b \right)}{\Delta(T^{-1})}.
 \end{aligned}
 \tag{7}$$

For CO adsorption in MFI (7) gives 3.5 kcal mol<sup>-1</sup>. Using the same method for fitting to the Langmuir–Freundlich model adsorption data taken from Calero and coworkers (2014), and the work by Golden and Sircar (1994) yields 3.6 and 3.9 kcal mol<sup>-1</sup>, respectively. Despite that the use the values from the adsorption isotherm to calculation of heat of adsorption is rather inaccurate, this result allows also to validate found isotherm. More reliable values was computed by the Widom test particle method (Frenkel and Smit 2002). It gives 3.9, 3.6 and 3.1 kcal mol<sup>-1</sup> for MFI, DDR and CHA, respectively. It is in reasonably good agreement with reported by Golden and Sircar (1994) and Savitz et al. (2000) 3.95 and 4 kcal mol<sup>-1</sup> from experiments, and computed by Calero and coworkers (2014) 4, 3.8 and 3.2 kcal mol<sup>-1</sup> values for MFI, DDR and CHA, respectively.

Figure 3 shows MS diffusivity calculated for CO from the slope of mean square displacement (4) and mean square displacement of the center of mass of the swarm of adsorbed molecules (5) respectively. MS diffusivity  $D_0$  is depends on loading, and can also be described using the Reed–Ehrlich quasi-chemical approach (Krishna et al. 2004):

$$D_0(\theta) = D_0(0) \frac{(1 + \epsilon)^{Z-1}}{(1 + \eta\epsilon)^Z},
 \tag{8}$$

where

$$\epsilon = \frac{\beta - 1 + 2\theta}{2\eta(1 - \theta)},
 \tag{9}$$

$$\beta = \sqrt{1 - 4\theta(1 - \theta)(1 - \eta)},
 \tag{10}$$

$$\eta = \exp \left( \frac{-w}{RT} \right),
 \tag{11}$$

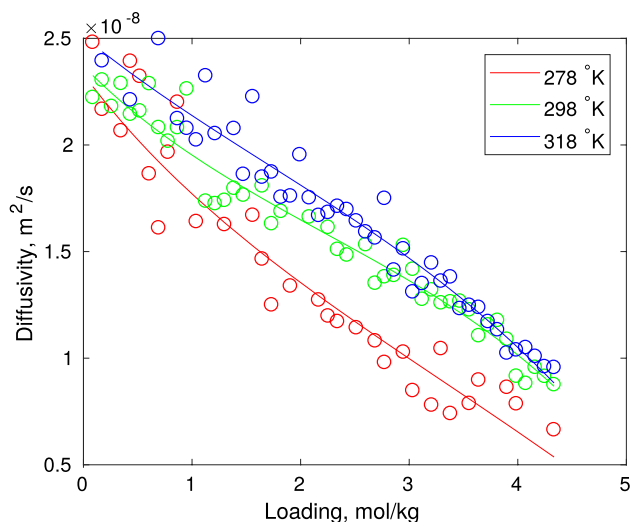


**Fig. 3** Maxwell–Stefan diffusivities in MFI at 278 K (red), 298 K (green) and 318 K (blue). Lines shows simulation data fitted to Reed–Ehrlich approximation (8) for Maxwell–Stefan diffusivity. (Color figure online)

$$\theta = \frac{c}{c_{sat}}, \quad (12)$$

$c_{sat}$  is the saturation capacity of species in a zeolite host,  $w$  is the interaction energy, which is affected by molecular interactions, and  $Z$  is the coordination number of the lattice, giving the number of nearest neighbours. For the MFI structure  $Z = 2.5$  (Krishna et al. 2007).

In this work, in line with (Krishna et al. 2007), we assume that the interaction energy depends on loading, and can be expressed as

$$\eta = a_1 \exp(-a_2 \theta). \quad (13)$$

The parameters after fitting the simulation data are given in Table 2. Despite adsorption isotherms drawn using these parameters are in the good agreement with simulation data, attempts to recover the values of the interaction energy using correspondence between Eqs. (11) and (13) are highly imprecise. Nevertheless, it can give a qualitative image of interaction energy. Supplementary Figure S5 shows the

curve of the dependence of interaction energy on the loading. It shows that interaction energy for CO in MFI, DDR and CHA has similar as (13) form.

The self-diffusion coefficient shown in Supplementary Figure S4 depends on the occupancy, and can be described by

$$D_{self}(c) = D_{self}(0) \exp(-ac), \quad (14)$$

where  $c$  is molar concentration of adsorbed CO and  $D_{self}(0)$  is self-diffusivity at zero loading.

Self-exchange coefficient  $D_{ii}$  shown in Fig. 4 represent molecule-molecule interaction and in case of diffusion in MFI additionally influenced by interaction with the walls (Mohammadi-Manesh et al. 2009). Comparing with Fuller, Schettler and Giddings (FSG) (Fuller et al. 1966) this values for the MFI a consistently lower than the fluid phase  $D_{ii}$ . This can indicate that carbon monoxide do not reach liquid phase in MFI crystal before saturation. Self-exchange diffusivity coefficient can be used in selectivity engineering for separation prediction. The binary exchange coefficients  $D_{12}$  reflect correlations in

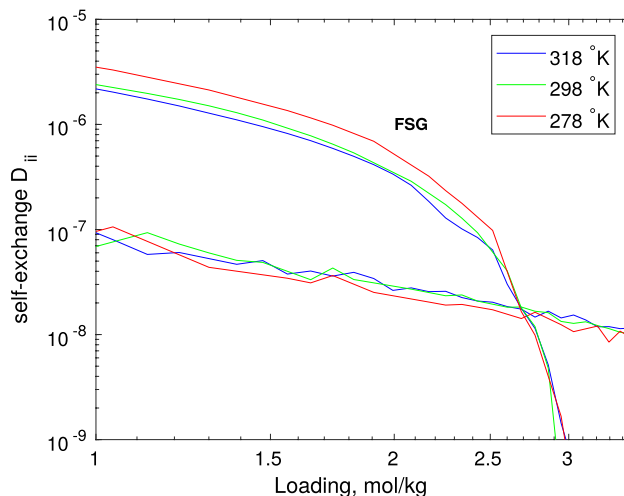


**Fig. 4** Self-exchange coefficient of CO diffusion in MFI at 278 K (red), 298 K (green) and 318 K (blue). To compare there are shown Fuller, Schettler and Giddings (FSG) lines. (Color figure online)

**Table 2** Reed–Ehrlich parameters for diffusivities of CO in MFI

	Self-diffusivity (14)		Reed–Ehrlich parameters (20) fitted to MD simulation data $\eta = a_1 \exp(-a_2 \theta)$			Reed–Ehrlich parameters (20) fitted to CBMC simulation data $\eta = a_1 \exp(-a_2 \theta)$		
	$D_{self}(0) = D_0(0)$ ( $10^{-8} \text{ m}^2 \text{ s}^{-1}$ )	$a$ ( $\text{kg mol}^{-1}$ )	$a_1$	$a_2$	$b$ ( $10^{-6} \text{ Pa}^{-1}$ )	$a_1$	$a_2$	$b$ ( $10^{-6} \text{ Pa}^{-1}$ )
278 K	2.3317	0.122	1.18	0.776	0.927	1.569	1.291	0.869
298 K	2.3697	0.103	1.56	0.908	0.621	1.234	0.993	0.590
318 K	2.5073	0.102	1.25	1.030	0.489	1.487	1.283	0.448

molecular jumps and can be estimated by empirical (Krishna and van Baten 2005, 2009) interpolation formula:

$$c_{2,sat}D_{12}^* = [c_{2,sat}D_{11}^*]^{c_1/(c_1+c_2)}[c_{1,sat}D_{22}^*]^{c_2/(c_1+c_2)} = c_{1,sat}D_{21}^* \tag{15}$$

where

$$\frac{c_{2,sat}}{c_1 + c_2}D_{12}^* = D_{12} = D_{21} = \frac{c_{1,sat}}{c_1 + c_2}D_{21}^* \tag{16}$$

The prediction of the  $D_{12}$  demands a lot of input data, including the  $c_{i,sat}$ , that are accessible from molecular simulations, but not commonly from experiments. Darken (1948) equation:

$$D_{12} = x_1D_{11} + x_2D_{22} \tag{17}$$

or adopted Vignes (1966) equation:

$$D_{12} = (D_{11})^{x_1}(D_{22})^{x_2} \tag{18}$$

where  $c_i$  are the molar concentrations defined in terms of the pore volume, and the  $x_i$  represent the component mole fractions  $x_i = c_i/c_t$ ,  $c_t$  is the total molar loadings. The estimation of  $D_{ij}$  is the key to the description of mixture diffusion characteristics; this parameter depends on a variety of factors: degree of confinement of the species within the pores, connectivity, and loading (Krishna and Baten 2009). As it has been marked in Krishna et al. (2004); Krishna and Baten (2009) either the Darken-type equation (17) or the Vignes-type equation (18) are to be preferred to the empirical interpolation formula (15) because of their more transparent physical basis. These equations allow estimation of the binary self-exchange coefficients for mixture diffusion from the unary self exchange. Using MS approach for modeling the performance of zeolite membranes in separations has proven to be useful. It allows to predict the mixture permeances based on single component adsorption and diffusion data as an input to the model. Using the above methodology and calculated parameters presented in this paper, one can use proven MS approach for modeling the productivity of zeolite membranes in separation of carbon monoxide from gas mixtures. Examples of using MS diffusivities and inverse of the thermodynamic factor to predict the Fick diffusivity can be found in Leppäjärvi et al. (2014); Ye et al. (2016).

The  $D_{ii}$  encapsulate the influence of correlation effects in unary diffusion. The larger the value of the MS diffusivity  $D_0$  with respect to self-exchange  $D_{ii}$  the stronger are the consequences of correlation effects, and we may consider the ratio  $D_0/D_{ii}$  as a measure of the degree of correlations. As depicted in Fig. 5 it can be fitted from the MD simulated data using the expression

$$\frac{D_0}{D_{ii}} = a_1 + a_2c \tag{19}$$

From simulation  $a_2 = 0.2749 \text{ kg mol}^{-1}$ ,  $a_1$  close to zero.

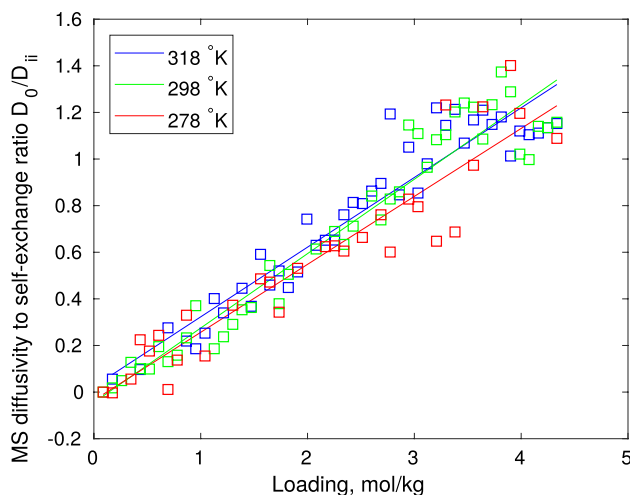


Fig. 5 MS diffusivity to self-exchange coefficient ratio for CO diffusion in MFI at 278 K (red), 298 K (green) and 318 K (blue). Lines show linear regression of data from simulation. (Color figure online)

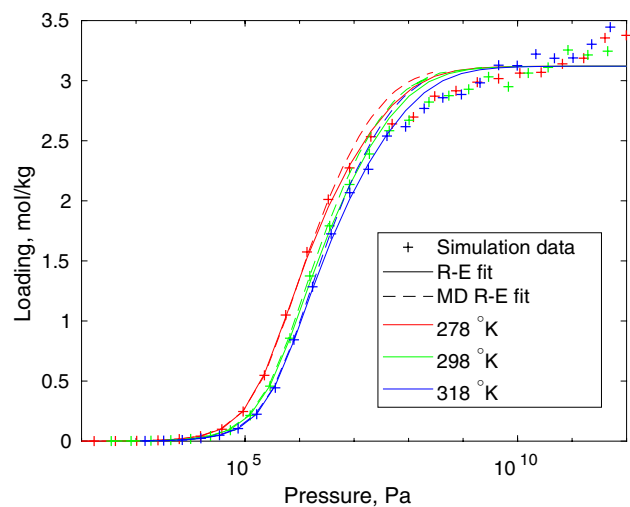


Fig. 6 Adsorption isotherms of CO in MFI-type zeolite (solid) at 278 K (red), 298 K (green) and 318 K (blue). Solid lines show Reed–Ehrlich approximation fit Dashed line shows Reed–Ehrlich adsorption isotherm with parameters calculated from fitting diffusion data. (Color figure online)

Inverse thermodynamic factor has been calculated using adsorption isotherm shown on Fig. 6 from fitted to simulation data Reed–Ehrlich (RE) approximation:

$$bP = \frac{\theta}{1 - \theta} \left( \frac{2 - 2\theta}{\beta + 1 - 2\theta} \right)^z \tag{20}$$

where  $b$  is RE parameter and in the low pressure region it reduces to the Henry law and  $b$  has same as Langmuir parameter temperature dependence

$$b = b_0 \exp\left(\frac{Q_{st}}{RT} \left(\frac{T_0}{T} - 1\right)\right) \quad (21)$$

At low occupancies region ( $bP \ll 1$ )  $c_{sat}bP = KP$ ,  $K$  is Henry's constant.

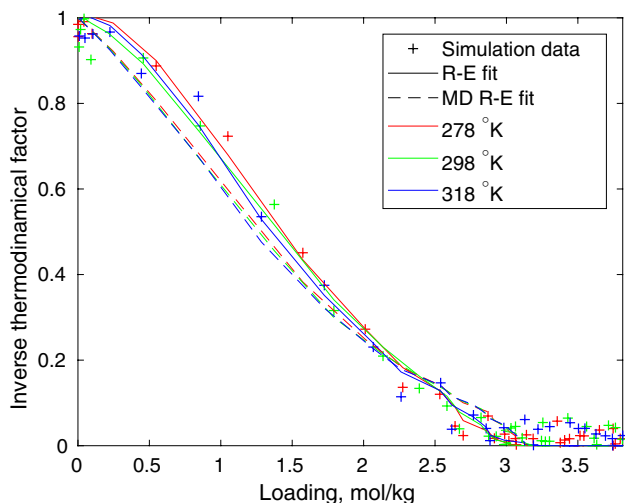


**Fig. 7** Inverse thermodynamical factor of CO in MFI-type zeolite (solid) at 278 K (red), 298 K (green) and 318 K (blue). Solid lines shows Reed–Ehrlich approximation fit. Dashed line shows thermodynamical factor from Reed–Ehrlich adsorption isotherm with parameters calculated from fitting diffusion data. (Color figure online)

Comparing it with simulated data one can see that RE approximation works for loading before saturation, when availability of free vacancies in near neighbourhood begin to play essential role.

Figure 4 shows that for loading more than  $2.7 \text{ mol kg}^{-1}$  carbon monoxide became in liquid phase, and according inverse thermodynamic factor on Fig. 7 Reed–Ehrlich approximation is inapplicable. According Fig. 5 in that area of loadings the ratio  $D_0/D_{ii}$  become valuable and, correspondently, correlation effects rises. As one can see in Fig. 3 the MS diffusion curve has a point of inflection near loading values close to the value where FSG curve cross the  $D_{ii}$  curve in Fig. 4. Starting with these loading values, the adsorption isotherm curve deviates from the single-site adsorption behaviors. By that reason adsorption isotherm has also been fitted for dual-site Langmuir–Freundlich model (Ruthven 1984) presented in Supplementary Figure S3. To examine the arrangements of CO in MFI at these conditions the average occupation profile of CO was reconstructed and shown in Fig. 8. The top-central part of Fig. 8 shows elliptic-shape occupation profiles, which is obtained by overlaying images of CO occurrences in the zigzag channels near intersections. Preferable adsorption sites of carbon monoxide are in the intersections and zigzag channels. Straight channels begins to be occupied in the saturation with high pressure. Self-diffusivity of car-

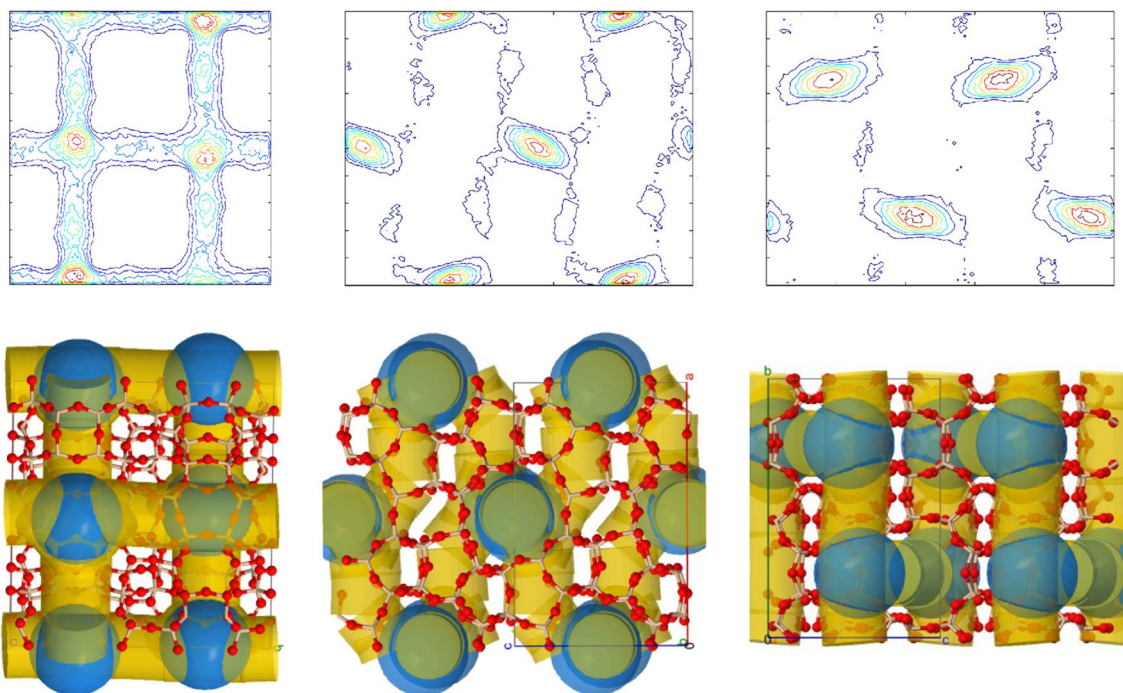


**Fig. 8** Average occupation profile for CO in MFI at 278 K and  $10^8 \text{ Pa}$ . Top row shows occupation isolines from left to right for 001, 010 and 100 crystallographic directions. Bottom row shows obtained from ZEOMICS site (First et al. 2011) view of MFI structure for illustrative purposes



bon monoxide through the MFI-type zeolite become steady with loading saturation.

## 4 Summary and conclusions

Molecular simulations were performed to explore at the microscopic scale the adsorption of CO in MFI, CHA and DDR. On the basis of classical force fields, Grand Canonical Monte Carlo simulations were performed for these types of zeolites up to high pressure to predict the adsorption properties and parameters for Langmuir–Freundlich, dual-side Langmuir–Freundlich and Toth isotherms were estimated. Using adsorption isotherm the isosteric enthalpy of adsorption has been calculated. It shows good agreement with available experimental data. Molecular dynamics simulation were run for MFI type of zeolite. Has been studied single component diffusion behaviours. Self-diffusion, Maxwell–Stefan diffusion and self-exchange coefficient has been examined according CO in MFI loading. In paper also summarized approach to use single component diffusion data in prediction of multicomponent diffusion. It has been shown applicability of Reed–Ehrlich approximation in diffusion and adsorption for CO in MFI. Using parameters for Reed–Ehrlich approximation obtained from diffusion data the adsorption isotherm and inverse thermodynamical factor has been examined and compared with adsorption from direct Monte-Carlo simulation. It shows good concordance one with other in the low and middle loading conditions. Self exchange diffusion coefficient examination shows that for high loadings CO arrive liquid phase where Reed–Ehrlich approximation should not work. For the pressure range  $10^2 - 10^8$  Pa that is of greatest interest in terms of practical use the Reed–Ehrlich model is proven to be useful. It has been shows that CO initially occupy the intersections and zig-zag channels in MFI, then with high loadings it begin to occupy straight channels. This paper gives enough data of adsorption and diffusivity of CO in MFI zeolites for using it in chemical process engineering. Using this data in appropriate model the steady-state sensitivity and dynamic stability analysis can be performed for separation subsystem in plant-wide perspective. It can be used to design of sustainable separation processes by means of systematic methods aided by computer simulation. This paper also shows limits of applicability for Reed–Ehrlich approximation. It has been shown that Reed–Ehrlich approximation can be used in the wide range of conditions presents main interest of the industry.

**Acknowledgements** The authors acknowledge the financial support from the Swedish Foundation for Strategic Research. The calculations were performed on resources provided by the Swedish National

Infrastructure for Computing (SNIC) at HPC2N. The study was also conducted as a part of a Russian Federation government project number 3628: Creation of the computing infrastructure for high-tech applications and Russian Foundation for Basic Research (RFBR) Project No. 16-29-15116.

**Open Access** This article is distributed under the terms of the Creative Commons Attribution 4.0 International License (<http://creativecommons.org/licenses/by/4.0/>), which permits unrestricted use, distribution, and reproduction in any medium, provided you give appropriate credit to the original author(s) and the source, provide a link to the Creative Commons license, and indicate if changes were made.

## References

- Ackley, M., Rege, S., Saxena, H.: Application of natural zeolites in the purification and separation of gases. *Microporous Mesoporous Mater.* **61**, 25–42 (2003)
- Allen, M., Tildesley, D.: *Computer Simulation of Liquids*. Clarendon Press, Oxford University Press Inc. and The American Chemical Society, Oxford (1989)
- Azizi, Z., Rezaeimanesh, M., Tohidian, T., Rahimpour, M.R.: Dimethyl ether: a review of technologies and production challenges. *Chem. Eng. Process.* **82**, 150–172 (2014)
- Baerlocher, C., McCusker, L.: Database of zeolite structures. <http://www.iza-structure.org/databases/> (2000). Accessed 26 June 2017
- Bernal, M.P., Coronas, J., Menéndez, M., Santamaría, J.: Separation of CO<sub>2</sub>/N<sub>2</sub> mixtures using MFI type zeolite membranes. *AIChE J.* **50**, 127–135 (2004)
- Bezus, A.G., Kiselev, A.V., Lopatkin, A.A., Du, P.Q.: Molecular statistical calculation of the thermodynamic adsorption characteristics of zeolites using the atom-atom approximation. Part 1. Adsorption of methane by zeolite NaX. *J. Chem. Soc. Faraday Trans.* **2**(74), 367–379 (1978)
- Caro, J., Noack, M.: Zeolite membranes—recent developments and progress. *Microporous Mesoporous Mater.* **115**, 215–233 (2008)
- Darken, L.: Diffusion, mobility and their interrelation through free energy in binary metallic systems. *Trans. Am. Inst. Min. Metall. Eng.* **175**, 184–201 (1948)
- Dragomirova, R., Wohrab, S.: Zeolite Membranes in Catalysis-From Separate Units to Particle Coatings. *Catalysts* **5**(4), 2161–2222 (2015). <https://doi.org/10.3390/catal5042161>
- Dubbeldam, D., Calero, S., Vlugt, T.J.H., Krishna, R., Maesen, T.L.M., Smit, B.: United atom force field for alkanes in nanoporous materials. *J. Phys. Chem. B* **108**(33), 12301–12313 (2004)
- Dubbeldam, D., Snurr, R.Q.: Recent developments in the molecular modeling of diffusion in nanoporous materials. *Mol. Simul.* **33**(4–5), 305–325 (2007)
- Einstein, A.: Über die von der molekularkinetischen Theorie der Wärme geforderte Bewegung von in ruhenden Flüssigkeiten suspendierten Teilchen. *Annalen der Physik* **17**, 549–560 (1905)
- Eller, K.R., Frederick, O.D.: *Encyclopedia of Chemical Technology: Carbon (cont'd) to cinchophen*. Interscience Encyclopedia, Incorporated, Oxford (1949)
- Feng, C., Khulbe, K., Matsuura, T., Farnood, R., Ismail, A.: Recent progress in zeolite/zeotype membranes. *J. Membr. Sci. Res.* **1**(2), 49–72 (2015)
- First, E.L., Gounaris, C.E., Wei, J., Floudas, C.A.: Computational characterization of zeolite porous networks: an automated approach. *Phys. Chem. Chem. Phys.* **13**(38), 17339–17358 (2011)

- Frenkel, D., Smit, B.: Understanding Molecular Simulations: From Algorithms to Applications, 2nd edn. Academic Press, San Diego (2002)
- Fuller, E.N., Schettler, P.D., Giddings, J.C.: New method for prediction of binary gas-phase diffusion coefficients. *Ind. Eng. Chem.* **58**(5), 18–27 (1966)
- García-Pérez, E., Parra, J., Ania, C., García-Sánchez, A., van Baten, J., Krishna, R., Dubbeldam, D., Calero, S.: A computational study of CO<sub>2</sub>, N<sub>2</sub>, and CH<sub>4</sub> adsorption in zeolites. *Adsorption* **13**(5–6), 469–476 (2007)
- Gądek, M., Kubica, R., Jędrzyk, E.: Production of Methanol and Dimethyl ether from biomass derived syngas – a comparison of the different synthesis pathways by means of flowsheet simulation, In: Kraslawski, A., Turunen, I. (eds) 23rd European symposium on computer aided process engineering, computer aided chemical engineering, vol. 32, pp. 55–60. Elsevier, New York (2013)
- Gilliam, O.R., Johnson, C.M., Gordy, W.: Microwave spectroscopy in the region from two to three millimeters. *Phys. Rev.* **78**, 140–144 (1950)
- Golden, T., Sircar, S.: Gas adsorption on silicalite. *J. Colloid Interface Sci.* **162**(1), 182–188 (1994)
- Grahn, M., Hedlund, J.: MaxwellStefan modeling of high flux tubular silicalite-1 membranes for CO<sub>2</sub> removal from CO<sub>2</sub>/H<sub>2</sub> gas mixtures. *J. Memb. Sci.* **471**, 328–337 (2014)
- Grande, C.A.: Advances in pressure swing adsorption for gas separation. *ISRN Chem. Eng.* **2012**, 982934 (2012)
- Guo, H., Zhu, G., Li, H., Zou, X., Yin, X., Yang, W., et al.: Hierarchical growth of largescale ordered zeolite silicalite 1 membranes with high permeability and selectivity for recycling CO<sub>2</sub>. *Angewandte Chemie* **118**, 7211–7214 (2006)
- Himeno, S., Tomita, T., Suzuki, K., Nakayama, K., Yajima, K., Yoshida, S.: Synthesis and permeation properties of a DDR-type zeolite membrane for separation of CO<sub>2</sub>/CH<sub>4</sub> gaseous mixtures. *Ind. Eng. Chem. Res.* **46**, 6989–6997 (2007)
- Hong, M., Li, S., Falconer, J.L., Noble, R.D.: Hydrogen purification using a SAPO-34 membrane. *J. Memb. Sci.* **307**, 277–283 (2008)
- Julbe, A., Motuzas, J., Cazevielle, F., Volle, G., Guizard, C.: Synthesis of sodalite/Al<sub>2</sub>O<sub>3</sub> composite membranes by microwave heating. *Sep. Purif. Technol.* **32**, 139–149 (2003)
- Kapteijn, F., Moulijn, J.A., Krishna, R.: The generalized MaxwellStefan model for diffusion in zeolites: sorbate molecules with different saturation loadings. *Chem. Eng. Sci.* **55**, 2923–2930 (2000)
- Khajavi, S., Jansen, J.C., Kapteijn, F.: Application of hydroxy sodalite films as novel water selective membranes. *J. Membr. Sci.* **326**, 153–160 (2009)
- Knoef, H.: Handbook Biomass Gasification. BTG Biomass Technology Group BV, Enschede (2005)
- Kosinov, N., Gascon, J., Kapteijn, F., Hensen, E.J.M.: Recent developments in zeolite membranes for gas separation. *J. Memb. Sci.* **499**, 65–79 (2016)
- Krishna, R.: Describing the diffusion of guest molecules inside porous structures. *J. Phys. Chem. C* **113**(46), 19756–19781 (2009)
- Krishna, R.: The MaxwellStefan description of mixture diffusion in nanoporous crystalline materials. *Microporous Mesoporous Mater.* **185**, 30–50 (2014)
- Krishna, R., van Baten, J.: The Darken relation for multicomponent diffusion in liquid mixtures of linear alkanes. An investigation using molecular dynamics (MD) simulations. *Ind. Eng. Chem. Res.* **44**(17), 6939–6947 (2005)
- Krishna, R., van Baten, J.: Unified MaxwellStefan description of binary mixture diffusion in micro- and meso-porous materials. *Chem. Eng. Sci.* **64**(13), 3159–3178 (2009)
- Krishna, R., van Baten, J.M., García-Pérez, E., Calero, S.: Incorporating the loading dependence of the Maxwell-Stefan diffusivity in the modeling of CH<sub>4</sub> and CO<sub>2</sub> permeation across zeolite membranes. *Ind. Eng. Chem. Res.* **46**, 2974–2986 (2007)
- Krishna, R., van der Broeke, L.: The Maxwell-Stefan description of mass transfer across zeolite membranes. *Chem. Eng. J.* **57**, 155–162 (1995)
- Krishna, R., Paschek, D., Baur, R.: Modeling the occupancy dependence of diffusivities in zeolites. *Microporous Mesoporous Mater.* **76**(1–3), 233–246 (2004)
- Kusakabe, K., Kuroda, T., Uchino, K., Hasegawa, Y., Morooka, S.: Gas permeation properties of ionexchanged faujasitetype zeolite membranes. *AIChE J.* **45**, 1220–1226 (1999)
- Kärger, J., Ruthven, D.M., Theodorou, D.N.: Diffusion in Nanoporous Materials. Wiley-VCH, Weinheim (2012)
- Leppäjärvi, T., Malinen, I., Korelskiy, D., Hedlund, J., Tanskanen, J.: MaxwellStefan modeling of ethanol and water unary pervaporation through a high-silica MFI zeolite membrane. *Ind. Eng. Chem. Res.* **53**, 323–332 (2014)
- Li, S., Falconer, J., Noble, R.: Improved SAPO 34 membranes for CO<sub>2</sub>/CH<sub>4</sub> separations. *Adv. Mater.* **18**, 2601–2603 (2006)
- Liquefaction of Gases, The Great Soviet Encyclopedia, 3rd edn, The Gale Group, Inc., Farmington Hills, (1970–1979)
- Liu, K., Song, C., Subramani, V.: Hydrogen and Syngas Production and Purification Technologies. Wiley-AIChE, New York (2010)
- Maple, J.R., Hwang, M.J., Stockfisch, T.P., Dinur, U., Waldman, M., Ewig, C.S., Hagler, A.T.: Derivation of class II force fields. I. Methodology and quantum force field for the alkyl functional group and alkane molecules. *J. Comput. Chem.* **15**(2), 162–182 (1994)
- Marschner, F., Moeller, F.: Methanol synthesis. In: Leach, B. (ed.) Applied Industrial Catalysis, vol. 2, pp. 215–243. Academic Press, New York (1983)
- Martin, M.G.: MCCCSTowhee: a tool for Monte Carlo molecular simulation. *Mol. Simul.* **39**(14–15), 1212–1222 (2013)
- Matito-Martos, I., Martín-Calvo, A., Gutierrez-Sevillano, J.J., Haranczyk, M., Doblare, M., Parra, J.B., Ania, C.O., Calero, S.: Zeolite screening for the separation of gas mixtures containing SO<sub>2</sub>, CO<sub>2</sub> and CO. *Phys. Chem. Chem. Phys.* **16**, 19884–19893 (2014)
- Mohammadi-Manesh, H., Alavi, S., Woo, T.K., Ashrafizaadeh, M., Najafi, B.: Molecular dynamics simulation of <sup>13</sup>C NMR powder lineshapes of CO in structure I clathrate hydrate. *Phys. Chem. Chem. Phys.* **11**, 8821–8828 (2009)
- Papadopoulos, G.K., Jobic, H., Theodorou, D.N.: Transport diffusivity of N<sub>2</sub> and CO<sub>2</sub> in silicalite: coherent quasielastic neutron scattering measurements and molecular dynamics simulations. *J. Phys. Chem. B* **108**(34), 12748–12756 (2004)
- Pałucha, S., Gburski, Z., Biesiada, J.: A molecular dynamics study of fullerene-carbon monoxide mixture. *J. Mol. Struct.* **704**(1–3), 269–273 (2004)
- Reed, D.A., Ehrlich, G.: Surface diffusion, atomic jump rates and thermodynamics. *Surf. Sci.* **102**, 588–609 (1981)
- Richardson, Y., Drobek, M., Julbe, A., Blin, J., Pinta, F.: Biomass gasification to produce syngas. In: Pandey, A., Bhaskar, T., Stöcker, M., Sukumaran, R.K. (eds.) Recent Advances in Thermo-Chemical Conversion of Biomass, pp. 213–250. Elsevier, Boston (2015)
- Ruthven, D.M.: Principles of Adsorption and Adsorption Processes. Wiley, New York (1984)
- Sandström, L., Sjöberg, E., Hedlund, J.: Very high flux MFI membrane for CO<sub>2</sub> separation. *J. Membr. Sci.* **380**, 232–240 (2011)
- Sato, K., Sugimoto, K., Nakane, T.: Mass-production of tubular NaY zeolite membranes for industrial purpose and their application to ethanol dehydration by vapor permeation. *J. Memb. Sci.* **319**, 244–255 (2008a)
- Sato, K., Sugimoto, K., Nakane, T.: Synthesis of industrial scale NaY zeolite membranes and ethanol permeating performance in pervaporation and vapor permeation up to 130 C and 570 kPa. *J. Membr. Sci.* **310**, 161–173 (2008b)

- Savitz, S., Myers, A.L., Gorte, R.J.: A calorimetric investigation of CO, N<sub>2</sub>, and O<sub>2</sub> in alkali-exchanged MFI. *Microporous Mesoporous Mater.* **37**, 33–40 (2000)
- Sethia, G., Bajaj, H.C., Somani, R.S.: *Adsorption Properties of Zeolites for Gas Separation. Separation by Zeolites*. LAP Lambert Academic Publishing, Germany (2013)
- Skoulidas, A.I., Sholl, D.S., Krishna, R.: Correlation effects in diffusion of CH<sub>4</sub>/CF<sub>4</sub> mixtures in MFI zeolite. A study linking MD simulations with the MaxwellStefan formulation. *Langmuir* **19**(19), 7977–7988 (2003)
- Smit, B.: Molecular simulations of the adsorption and diffusion of hydrocarbons in molecular sieves. In: Xu, R., Gao, Z., Chen, J., Yan, W. (eds.) *From zeolites to porous MOF materials—the 40th anniversary of international zeolite conference*, vol. 170, pp. 121–128 (2007)
- Taylor, R., Krishna, R.: *Multicomponent Mass Transfer*. Wiley, New York (1993)
- Todorov, I., Smith, W.: The dl\_poly user manual version 4.02.0. [http://www.ccp5.ac.uk/DL\\_POLY/](http://www.ccp5.ac.uk/DL_POLY/) (2011). Accessed 26 June 2017
- Tomita, T., Nakayama, K., Sakai, H.: Gas separation characteristics of DDR type zeolite membrane. *Microporous Mesoporous Mater.* **68**, 71–75 (2004)
- van den Bergh, J., Zhu, W., Gascon, J., Moulijn, J.A., Kapteijn, F.: Separation and permeation characteristics of a DD3R zeolite membrane. *J. Memb. Sci.* **316**, 35–45 (2008)
- Vignes, A.: Diffusion in binary solutions. *Ind. Eng. Chem. Fundam.* **5**, 189–199 (1966)
- Ye, P., Grahn, M., Korelskiy, D., Hedlund, J.: Efficient separation of N<sub>2</sub> and he at low temperature using MFI membranes. *AIChE J.* **62**, 2833–2842 (2016)